Benzo-Bridged Bis(1,2,3-dithiazoles) and Their Selenium Analogues. Preparation, Molecular and Electronic Structures, and Redox Chemistry

T. M. Barclay,[1a] A. W. Cordes,[1a] J. D. Goddard,[1b] R. C. Mawhinney,[1b] R. T. Oakley,*,[1b] K. E. Preuss,[1b] and R. W. Reed[1b]

Contribution from the Department of Chemistry and Biochemistry, University of Arkansas, Fayetteville, Arkansas 72701, and Department of Chemistry and Biochemistry, University of Guelph, Guelph, Ontario N1G 2W1 Canada
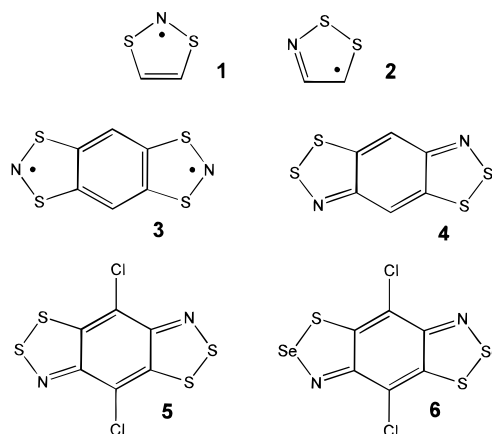
Received August 19, 1997[⊗]

Abstract: The condensation of diaminobenzenedithiol with sulfur monochloride leads to the chloride salt of the radical cation of 3,6-dichlorobenzo[1,2-*d*:4,5-*d'*]bis(1,2,3-dithiazole), dichloro-[BB-123-DTA][Cl], which can be reduced to neutral dichloro-[BB-123-DTA] with triphenylantimony. A similar condensation with selenium tetrachloride leads, upon reduction, to the corresponding bis(1,2,3-thiaselenazole) dichloro-[BB-123-TSA]. The crystal and molecular structures of both compounds have been determined by X-ray diffraction. Both compounds, which are formally antiaromatic 16π-systems, exhibit internal bond lengths consistent with a quinoid formulation. The radical cations of both rings have been characterized by ESR spectroscopy; for dichloro-[BB-123-DTA]$^+$ $g = 2.0114$ and $a_N = 0.201$ mT, while for dichloro-[BB-123-TSA]$^+$ $g = 2.021$ and $a_N = 0.44$ mT. Further oxidation of both rings affords the corresponding dications, both of which have been characterized crystallographically as their AlCl$_4^-$ salts. The structural features of these compounds are consistent with those expected for dithiazolylium (or thiaselenazolylium) derivatives. The structure and redox chemistry of the benzo[1,2-*d*:4,5-*d'*]bis(1,2,3-dithiazole) framework is discussed in the light of the results of *ab initio* calculations.

Introduction

Neutral heterocyclic radicals based on both the 1,3,2- and 1,2,3-dithiazolyl (DTA) ring systems **1** and **2** have been known for many years.[2−4] While the solid state structures of several monofunctional 1,3,2-derivatives[5] and also the diradical benzobis(1,3,2-dithiazolyl) [BB-132-DTA] **3** have been characterized,[6] the solid state fate of even simple 1,2,3-DTAs is unknown. In order to learn more of the structural and redox properties of 1,2,3-DTAs, we have pursued the characterization of derivatives based on the bifunctional heterocycle benzo[1,2-*d*:4,5-*d'*]bis-

(1,2,3-dithiazole) or [BB-123-DTA]. While a diradical formulation akin to **3** can be drawn for this compound, the quinoid representation **4** is more likely. Herein we report the preparation
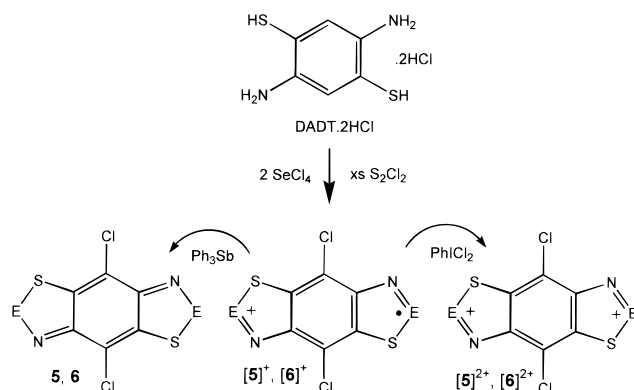

and structural characterization of two compounds based on **4**, namely the dichloro derivative **5** and its thiaselenazole analogue **6**. The redox chemistry of these rings has also been investigated; sequential oxidation affords the radical cations [**5**]$^+$/[**6**]$^+$ and the dications [**5**]$^{2+}$/[**6**]$^{2+}$. The former have been characterized by ESR spectroscopy and the latter by X-ray crystallography (as their AlCl$_4^-$ salts). *Ab initio* calculations of the energies, ionization potentials, and electron affinities of the quinoid singlet and triplet states of **4** have been performed, and the results are used to compare the redox chemistry and structures of bifunctional 1,2,3- and 1,3,2-DTAs.

Results and Discussion

Synthesis. The most common preparative route to the 1,2,3-dithiazolylium ring system is the Herz reaction, *i.e.*, the

⊗ Abstract published in *Advance ACS Abstracts,* December 1, 1997.

(1) (a) University of Arkansas. (b) University of Guelph.

(2) (a) Awere, E. G.; Burford, N.; Mailer, C.; Passmore, J.; Schriver, M. J.; White, P. S.; Banister, A. J.; Oberhammer, A. J.; Sutcliffe, L. H. *J. Chem. Soc., Chem. Commun.* **1987,** 66. (b) MacLean, G. K.; Passmore, J.; Rao, M. N. S.; Schriver, M. J.; White, P. S. *J. Chem. Soc., Dalton Trans.* **1985,** 1405. (c) Wolmershäuser, G.; Kraft, G. *Chem. Ber.* **1989,** *122,* 385. (d) Harrison, S. R; Pilkington, R. S.; Sutcliffe, L. H. *J. Chem. Soc., Faraday Trans. I* **1984,** *80.* 669. (f) Fairhurst, S. A.; Pilkington, R. S.; Sutcliffe, L. H. *J. Chem. Soc., Faraday Trans. I* **1983,** *79,* 439. (g) Fairhurst, S. A.; Pilkington, R. S.; Sutcliffe, L. H. *J. Chem. Soc., Faraday Trans. I* **1983,** *79,* 925.

(3) Preston, K. F.; Sutcliffe, L. H. *Magn. Reson. Chem.* **1990,** *28,* 189.

(4) (a) Mayer, R.; Domschke, G.; Bleisch, S. *Tetrahedron Lett.* **1978,** 4003. (b) Mayer, R.; Domschke, G.; Bleisch, S.; Bartl, A; Stǎsko, A. *Z. Chem.* **1981,** *21,* 146, 264. (c) Mayer, R.; Domschke, G.; Bleisch, S.; Fabian, J.; Bartl, A;. Stǎsko, A. *Collect. Czech. Chem. Commun.* **1984,** *49,* 684. (d) Mayer, R.; Bleisch, S.; Domschke, G.; Tkáč, A.; Stǎsko, A. *Org. Magn. Reson.* **1979,** *12,* 532. (e) Harrison, S. R.; Pilkington, R. S.; Sutcliffe, L. H. *J. Chem. Soc., Faraday Trans. I* **1984,** *80,* 669.

(5) (a) Barclay, T. M.; Cordes, A. W.; George, N. A.; Haddon, R. C.; Oakley, R. T.; Palstra, T. T. M.; Patenaude, G. W.; Reed, R. W.; Richardson, J. F.; Zhang, H. *J. Chem. Soc., Chem. Commun.* **1997,** 873. (b) Wolmershäuser, G.; Kraft, G. *Chem. Ber.* **1990,** *123,* 881. (c) Awere, E. G.; Burford, N.; Haddon, R. C.; Parsons, S.; Passmore, J.; Waszczak, J. V.; White, P. S. *Inorg. Chem.* **1990,** *29,* 4821. (d) Wolmershäuser, G.; Johann, R. *Angew. Chem., Int. Ed. Engl.* **1989,** *28,* 920.

(6) Barclay, T. M.; Cordes, A. W.; de Laat, R. H.; Goddard, J. D.; Haddon, R. C.; Jetter, D. Y.; Mawhinney, R. C.; Oakley, R. T.; Palstra, T. T. M.; Patenaude, G. W.; Reed, R. W.; Westwood, N. P. C. *J. Am. Chem. Soc.* **1997,** *119,* 2633.

Scheme 1

Figure 1. X-band ESR spectrum of [**5**]$^+$ in SO_2(l); sweep width 5 mT.

cyclocondensation of an aromatic amine with sulfur monochloride.[7] This approach fails when applied to p-phenylenediamine, which does not react with sulfur monochloride. However, the condensation of diaminobenzenedithiol dihydrochloride (DADT·2HCl) with sulfur monochloride is more fruitful (Scheme 1). When carried out at reflux in neat sulfur monochloride, the chloride salt of the radical cation [**5**]$^+$ is formed in good yield. Reduction of this salt with triphenylantimony affords the neutral heterocycle **5** as an air-stable, purple/black crystalline solid that is sparingly soluble in chlorobenzene, and which sublimes at 160 °C/10^{-3} Torr. The selenium-based derivative can be generated using a similar approach, *i.e.*, the condensation of selenium tetrachloride and DADT·2HCl in refluxing chlorobenzene. Reduction of [**6**][Cl] yields the neutral compound **6**, which can be recrystallized from hot benzonitrile as lustrous green flakes. Sublimation at 190 °C/10^{-3} Torr then affords green/gold blocks. Chlorination of the benzene ring during the course of both these condensations appears to be unavoidable. When a deficit of S_2Cl_2/$SeCl_4$ is employed, a mixture of the chlorinated material, along with unreacted DADT·2HCl, is formed.

The production of the radical cations [**5**]$^+$/[**6**]$^+$ rather than the dications [**5**]$^{2+}$/[**6**]$^{2+}$ in these condensation reactions was unexpected. Under relatively mild oxidizing conditions the isomeric ring system **3** is oxidized directly to [**3**]$^{2+}$. By contrast, **5** reacts only slowly with chlorine, leading not to [**5**]$^{2+}$ but to materials which, by mass spectral evidence, appear to have undergone S–S bond cleavage and ring degradation. Oxidation of [**5**] to the radical cation salt [**5**][Cl] can be effected by heating the neutral material in chlorobenzene solution with excess sulfur dichloride. Treatment of [**5**][Cl] with $AlCl_3$ in liquid SO_2 affords the corresponding tetrachloroaluminate salt as a black, sparingly soluble, crystalline solid. Further oxidation of [**5**]-[Cl] with $PhICl_2$ or SO_2Cl_2 in the presence of $AlCl_3$ in liquid SO_2 then affords the closed shell dicationic salt [**5**][AlCl$_4$]$_2$. Analogous chemistry can be effected with the selenium containing compound **6**. In order to test the ease of comproportionation of the neutral and dicationic states a mixture of **5** and [**5**][AlCl$_4$]$_2$ was slurried in liquid SO_2 for several hours. Subsequent filtration and infrared analysis of the product revealed the exclusive formation of [**5**][AlCl$_4$].

Cyclic Voltammetry. The resistance of **5** to chemical oxidation is in contrast to the behavior of simple 1,2,3-dithiazolyls. We have therefore examined its electrochemical properties to gain more quantitative insight into the redox properties of this system. Cyclic voltammetry on **5** in CH_3CN (with Pt electrodes and 0.1 M n-Bu$_4$NPF$_6$ as supporting electrolyte, ref. SCE) reveals a reversible oxidation wave with $E_{1/2}$(ox) = 0.93 V and a second, irreversible oxidation process
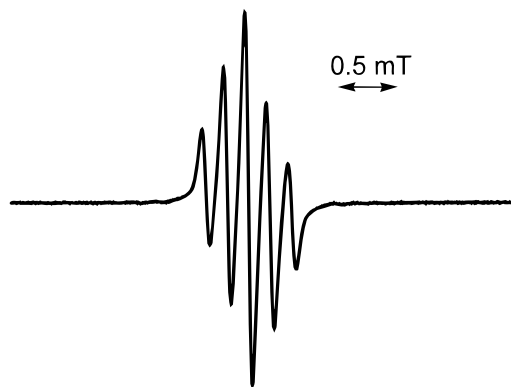
with an anodic peak potential E_{pa} = 1.5 V. These potentials are significantly higher than those found for the oxidation of a simple 1,2,3-dithiazolyls, *e.g.*, benzo-1,2,3-dithiazolyl ($E_{1/2}$(ox) = 0.26 V),[8] or the isomeric heterocycle **3** ($E_{1/2}$(ox) = 0.16 V).[6] Attempts to suppress the irreversibility of the [**5**]$^+$/[**5**]$^{2+}$ couple by varying the voltage sweep rate and substrate concentrations were unsuccessful. We attribute the electrochemical irreversibility of this chemically reversible reaction to the rapid comproportionation of [**5**]$^{2+}$ with excess **5**. Reduction of **5** occurs via a single, broad and strongly irreversible wave with a cathodic peak potential E_{pc} = −0.95 V.

ESR Spectra. While solutions of the neutral compounds **5** and **6** are ESR silent, as would be expected of a quinoid ground state, solutions of the radical cations (as the AlCl$_4^-$ salts) in liquid SO_2 exhibit extremely strong and persistent ESR signals. For both [**5**]$^+$ and [**6**]$^+$ the ESR spectra consist of 1:2:3:2:1 quintets (Figure 1), confirming that spin density is fully delocalized over both nitrogen atoms. The effects of spin-orbit coupling (at sulfur) on the g-value are more pronounced in [**5**]$^+$ than in simple monofunctional dithiazolyls, and, consistently, the observed g-value of 2.0114 is larger than in, for example, benzo-1,2,3-dithiazolyl (g = 2.008).[4] Likewise, the more extensive delocalization of spin density in [**5**]$^+$ relative to simple 1,2,3-dithiazolyls leads to a smaller hyperfine coupling constant at nitrogen (a_N = 0.201 mT). That the g-value is larger, and the a_N value smaller, than in the isomeric (albeit unchlorinated) radical cation [**3**]$^+$ (g = 2.0068, a_N = 0.624 mT)[9] suggests a heavier spin density on sulfur (*vide infra*). In [**6**]$^+$ the g-value is increased to 2.0211, as expected from the incorporation of the heavier chalcogen. The a_N value, however, also increases to 0.44 mT, in accord with the previously observed tendency of selenium (relative to sulfur) to partition spin density onto a neighboring nitrogen.[10]

Crystal Structures. Crystals of **5** and **6** suitable for X-ray crystallography were grown by fractional sublimation *in vacuo*. Crystals of [**5**][AlCl$_4$]$_2$ and [**6**][AlCl$_4$]$_2$ were grown by slow evaporation of SO_2/$SOCl_2$ solutions.[11] Crystal data are compiled in Table 1. PLUTO drawings of the crystal packing of the two neutral molecules are illustrated in Figure 2. Table 2 provides a summary of the pertinent intramolecular bond lengths in all four structures.

(7) Warburton, W. K. *Chem. Rev.* **1957**, *57*, 1011.

(8) Tsveniashvili, V. Sh.; Malashkiya, M. V. *Elektrokim.* **1984**, *3*, 357.
(9) (a) Dormann, E.; Nowak, M. J.; Williams, K. A.; Angus, R. O., Jr.; Wudl, F. *J. Am. Chem. Soc.* **1987**, *109*, 2594. (b) Wolmershäuser, G.; Schnauber, M.; Wilhelm, T.; Sutcliffe, L. H. *Synth. Met.* **1986**, *14*, 239.
(10) (a) Bestari, K.; Cordes, A. W.; Oakley, R. T.; Young, K. M. *J. Am. Chem. Soc.* **1990**, *112*, 2249. (b) Oakley, R. T.; Reed, R. W.; Cordes, A. W.; Craig, S. L.; Graham, S. B. *J. Am. Chem. Soc.* **1987**, *109*, 7745.
(11) X-ray data were also collected on crystals of the radical cation salt [**5**][AlCl$_4$]. However, severe disorder of the radical cation in the observed trigonal space group precluded a refinement below a R-value of 0.2.

Table 1. Crystal Data

formula	$S_4N_2C_6Cl_2$	$S_4N_2C_6Cl_{10}Al_2$	$Se_2S_2N_2C_6Cl_2$	$Se_2S_2N_2C_6Cl_{10}Al_2$
fw	299.22	636.81	393.02	730.61
a, Å	3.8496(10)	7.2015(6)	7.478(4)	9.1189(13)
b, Å	7.9577(7)	7.2286(9)	3.9733(17)	12.0258(19)
c, Å	15.5280(18)	11.2841(10)	15.875(9)	9.8823(10)
α, deg		104.746(9)		
β, deg	95.963(14)	100.965(8)	90.33(4)	92.368(10)
γ, deg		99.638(8)		
V, Å^3	473.11(14)	543.09(9)	471.7(4)	1082.8(3)
ρ_{calcd}, g cm^{-3}	2.10	1.95	2.76	2.24
space group	$P2_1/c$	$P\bar{1}$	$P2_1/n$	$P2_1/c$
Z	2	1	2	2
radiation	MoKα, graphite monochromated	MoKα, graphite monochromated	MoKα, graphite monochromated	MoKα, graphite monochromated
λ, Å	0.7107	0.7107	0.7107	0.7107
temp, K	293	293	293	293
μ, mm^{-1}	1.49	1.74	8.80	4.89
refls in refinement	926	1474	921	927
$R(F)$, $R_w(F)^a$	0.038, 0.032	0.041, 0.054	0.089, 0.216	0.057, 0.071

$^a R = [\Sigma||F_o| - |F_c||]/[\Sigma|F_o|]$; $R_w = \{[\Sigma w||F_o| - |F_c||^2]/[\Sigma(w|F_o|^2)]\}^{1/2}$.
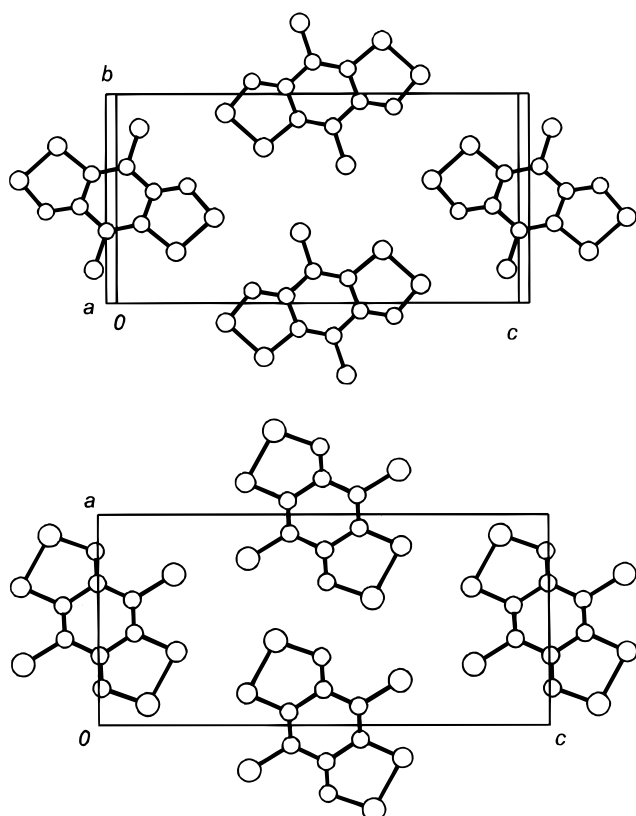
Figure 2. Packing patterns of **5** (above) and **6** (below).

Table 2. Summary of Intramolecular Bond Lengths (in Å)

bond^a	**5**	[**5**][AlCl$_4$]$_2$	**6**	[**6**][AlCl$_4$]$_2$
E−S	2.0904(9)	2.0285(18)	2.248(4)	2.136(5)
E−N	1.638(2)	1.567(4)	1.783(11)	1.735(11)
S−C	1.737(2)	1.724(4)	1.727(13)	1.702(14)
N−C	1.306(3)	1.349(6)	1.300(16)	1.356(18)
(N)C−C(Cl)	1.432(3)	1.397(6)	1.436(17)	1.40(2)
(N)C−C(S)	1.457(3)	1.436(6)	1.476(17)	1.45(2)
(S)C−C(Cl)	1.356(3)	1.381(7)	1.346(19)	1.40(2)
Cl−C	1.720(2)	1.694(4)	1.749(13)	1.689(14)

^{a} E = S (**5**) or Se (**6**).

Compounds **5** and **6** belong to the monoclinic space groups $P2_1/c$ and $P2_1/n$, respectively. Both molecules lie on crystallographic inversion centers and are essentially planar to within 0.02 and 0.06 Å, respectively. In both **5** and **6** the molecules adopt slipped π-stack structures, not unlike that observed for

3,[6] with cell repeats along the stacking axis of 3.8496(10) and 3.9733(17) Å. The packing patterns adopted by these slipped stacks is, however, quite different (Figure 2). In **5**, adjacent molecules approach one another in a side-on manner, while those of **6** are packed in more of a head-to-head fashion. The structures of [**5**][AlCl$_4$]$_2$ and [**6**][AlCl$_4$]$_2$ belong to the space groups $P\bar{1}$ and $P2_1/c$, respectively, and consist of relatively discrete dications and AlCl$_4^-$ counter anions. As in the neutral compounds the dications lie on a center of symmetry and are essentially encapsulated within the superstructure afforded by the AlCl$_4$- ions, so that there are no unusually short interannular contacts between neighboring rings. Both dication molecules are planar to within 0.03 Å.

In agreement with the fact that both **5** and **6** are ESR inactive, the intramolecular distances in both compounds fall into patterns consistent with a closed-shell quinoid formulation. The variation in the C−C bonds is nonetheless not quite as pronounced as in, for example, *p*-benzoquinone-*N,N′*-bis(methylsulfonyldiimine), **7**.[12] The pattern is, indeed, very similar to that observed in the 1,4-phenylene bridged bis(1,3,2,4-dithiadiazolyl) **8**,[13] which exists in the solid state as an associated diradical. Upon oxidation of both **5** and **6** to the dicationic state the bond lengths in both the heterocyclic and benzene rings change considerably. The (N)C−C(Cl) and (S)C−C(Cl) bonds become essentially equivalent, denoting loss of the quinoid formulation, while the S−S, S−N, and N−C bond distances in [**5**][AlCl$_4$]$_2$ evolve to values which are very similar to those found in simple benzo-1,2,3-dithiazolylium salts.[14]
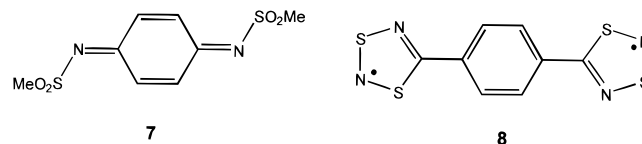
Electronic Structure Calculations. Recently we reported the results of HF/cep-31+g** level calculations on the geometries, ionization potentials (IPs), and electron affinities (EAs) of the [BB-132-DTA] system **3**.[6] We have since extended these calculations to include electron correlation via the DFT scheme,

(12) Švets, A. E.; Mišnev, A. F.; Bleidelis, J. J. *J. Struct. Chem.* **1983**, *19*, 473.
(13) Banister, A. J.; Rawson, J. M.; Clegg, W.; Birkby, S. L. *J. Chem. Soc., Dalton Trans.* **1991**, 1099.
(14) Bats, J. W.; Fuess, H.; Weber, K. L.; Roesky, H. W. *Chem. Ber.* **1983**, *116*, 1751.

Table 3. Total[a] Energies (Hartree) of [BB-132-DTA] **3** and [BB-123-DTA] **4** as a Function of Oxidation State[b]

compd	state	energy	compd	state	energy
[**3**]$^{2+}$	$^1A_{1g}$	−95.051 32 (19.53)	[**4**]$^{2+}$	^1A_g	−95.089 05 (18.50)
[**3**]$^+$	$^2B_{1u}$	−95.462 38 (8.34)	[**4**]$^+$	^2A_u	−95.514 71 (6.92)
3	$^1A_{1g}$	−95.686 70 (2.24)	**4**	^3B_u	−95.742 34 (0.72)
	$^3B_{2u}$	−95.704 19 (1.76)		^1A_g	−95.768 98 (0.00)
[**3**]$^-$	^2A	−95.756 98 (0.33)	[**4**]$^-$	^2A	−95.792 01 (−0.63)

[a] Energies correspond to B3LYP/dcep-31g* geometries optimized in D_{2h} and C_{2h} symmetry (C_1 symmetry in the case of the two radical anions). [b] Relative energies (eV) in parentheses.

Table 4. Summary of Bond Lengths[a] (Å), Net Atomic Charges[b] (q) of [BB-123-DTA] **4** and Its Corresponding Radical Cation and Dication

	4			
state	^1A_g	^3B_u	[**4**]$^+$ ^2A_u	[**4**]$^{2+}$ ^1A_g
S−S	2.158	2.150	2.124	2.095
S−N	1.663	1.647	1.621	1.586
S−C	1.769	1.776	1.754	1.748
N−C	1.319	1.385	1.341	1.359
(N)C−C(H)	1.450	1.418	1.433	1.424
(N)C−C(S)	1.483	1.439	1.390	1.467
(S)C−C(H)	1.377	1.404	1.390	1.402
q_N	−0.57	−0.60	−0.53	−0.47
$q_{S(N)}$	0.43	0.50	0.67	0.89
$q_{S(C)}$	0.19	0.19	0.34	0.49
$q_{C(N)}$	0.15	0.08	0.14	0.13
$q_{C(S)}$	−0.19	−0.21	−0.20	−0.21
$q_{C(H)}$	−0.26	−0.21	−0.20	−0.13

[a] B3LYP/dcep-31g* optimized geometries in C_{2h} symmetry. [b] B3LYP/IGLO-III//B3LYP/dcep-31g* natural population analysis.

Table 5. Calculated (B3LYP/IGLO-III//B3LYP/dcep-31g*) Spin Densities (ρ) and Isotropic Hyperfine Coupling Constants a_N (mT) for the Radical Cations [**3**]$^+$ and [**4**]$^+$

	ρ_N	$\rho_{S(N)}$	$\rho_{S(C)}$	$\rho_{C(N)}$	$\rho_{C(S)}$	$\rho_{C(H)}$	a_N
[**3**]$^+$	0.354	0.070	0.070		−0.047	0.106	0.623
[**4**]$^+$	0.128	0.265	0.089	−0.055	−0.028	0.106	0.219

and herein we compare these new results with those obtained at the same level of theory on the isomeric compound **4**, the parent of the dichloro-derivative **5**. Relative energies of the two isomers in various oxidation states are listed in Table 3. A summary of intramolecular distances in the [BB-123-DTA] **4**, as a function of oxidation state, is provided in Table 4, and computed spin densities and ^{14}N hyperfine coupling constants in the radical cations [**3**]$^+$ and [**4**]$^+$ are listed in Table 5.

The interpretation of the computational results is facilitated with reference to a simple molecular orbital picture of the frontier molecular orbital (FMO) manifolds of the two systems. These can be developed in terms of the fusion of two DTA radicals (1,2,3- or 1,3,2-) to a central benzene nucleus. Mixing of the singly occupied molecular orbitals (SOMOs) of the radicals with the π-system of benzene leads to the combinations shown in Figure 3. In each case the 16π-electron system so produced can exist in several configurations. If orbital mixing is weak, a diradical state will arise. If it is strong, an "antiaromatic" quinoidal singlet is formed. While the bis-1,3,2-system is not formally disjoint,[15,16] the two frontier orbitals b_{1u} and b_{3g} are nonetheless sufficiently close in energy that the

(15) (a) Borden, W. T.; Davidson, E. R. *J. Am. Chem. Soc.* **1977**, *99*, 4587. (b) Pranata, J.; *J. Am. Chem. Soc.* **1992**, *114*, 10537. (c) Racja, A. *Chem. Rev.* **1994**, *94*, 871.

(16) (a) Borden, W. T. In *Diradicals*; Borden, W. T., Ed.; J. Wiley and Sons: New York, 1982; p 24. (b) Salem, L. *Electrons in Chemical Reactions; First Principles*; Wiley Interscience: Chichester, U. K., 1982; Chapter 3. (c) Salem, L.; Rowland, C. *Angew. Chem., Int. Ed. Engl.* **1972**, *11*, 92.
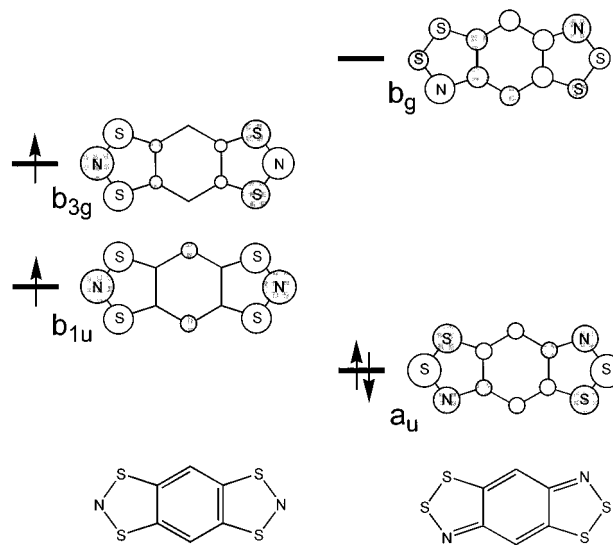
Figure 3. Qualitative frontier orbital pictures of **3** and **4**.
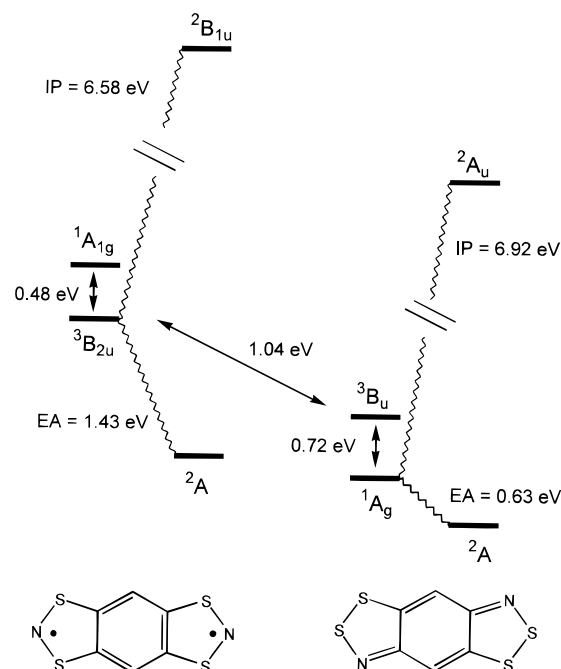
Figure 4. Relative energies (eV) of **3** and **4**, their anions, and cations.

system is diradical, with the energies of the triplet and open shell singlet states being within 1 kcal/mol of each other. The closed shell singlet $^1A_{1g}$ lies 0.48 eV above the triplet $^3B_{2u}$ (Figure 4). By contrast the asymmetry of the pairwise combinations of 1,2,3-DTA SOMOs leads, upon mixing with benzene, to a much greater splitting of the two frontier orbitals a_u and b_g, and a quinoid singlet ground state for **4**. Of the two isomers, the bis-1,2,3-variant is more stable. The diradical triplet ^3B_u for **4** is predicted to lie 0.72 eV above the singlet ground state, and this triplet is, in turn, more stable than the corresponding $^3B_{2u}$ triplet of **3** by 1.04 eV.

Comparison of the geometries of the singlet and triplet states of [BB-123-DTA] reveals major changes in the N−C bonds and, to lesser extents, the C−C bonds, that occur as the structure switches from a quinoid to diradical formulation. In simple FMO terms these changes follow naturally from the promotion of an electron from the a_u to b_g orbital (Figure 3). The structural evolution accompanying the oxidation and reduction of **4** can be easily interpreted using the same frontier orbital framework. Sequential oxidation removes electrons from the a_u orbital, leading to a progressive shortening of the S−S and S−N bonds,

lengthening of the N−C bond, and the equalization of the benzene C−C bonds (Table 4). All the distances map very smoothly onto those seen in the crystal structures of [**5**] and [**5**][AlCl$_4$]$_2$ (Table 2). Interestingly, reduction of **4** to [**4**]$^-$ places an electron in the b$_g$ orbital, which is strongly antibonding over the N−S linkage. As a result, full geometry optimization leads to cleavage of one of the N−S bonds and a lowering of symmetry from C_{2h} to C_1. The ensuing structure, which remains approximately planar, is well described by the valence bond representation **9**, *i.e.*, an acyclic radical anion.

9
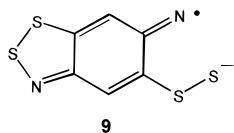
From an energetic perspective the relatively high IP (6.92 eV) and low EA (0.63 eV) of **4** (Figure 4) can also be understood in simple FMO terms. As a result of the larger FMO separation found in the quinoid ground state of **4** should be far more resistant to both oxidation and reduction than the triplet ground state of the bis-1,3,2-variant **3**. Consistently the disproportionation energy ΔH_{disp} (= IP − EA) for **4** (6.29 eV) is significantly larger than for **3** (5.14 eV). By contrast, disproportionation of the radical cations to the corresponding neutrals and dications is energetically very similar; for [**4**]$^+$ ΔH_{disp} = 4.66 eV, while for [**3**]$^+$ ΔH_{disp} = 4.61 eV. In accord with the differences in the ESR g-values and hyperfine coupling constants observed for [**5**]$^+$ and [**6**]$^+$, the calculated spin distributions (Table 5) reveal a significant shift of spin density from nitrogen to sulfur in [**4**]$^+$. The calculated[17] isotropic ^{14}N hyperfine coupling constants follow suit and are in remarkably close agreement with experiment.

Summary and Conclusions

The antiaromatic heterocycles 3,6-dichlorobenzo[1,2−*d*:4,5−*d*′]bis(1,2,3-dithiazole) **5** and its selenium analogue **6** display a rich redox chemistry. Neither are particularly strong donors, indeed they are relatively weak in comparison to typical organic π-donors (*e.g.*, tetrathiafulvalene),[18,19] but the radical cation states [**5**]$^+$ and [**6**]$^+$ are extremely stable with respect to disproportionation. The ease of preparation of simple salts of these radical cations augurs well for their use in the design of new molecular conductors (for [**5**][AlCl$_4$] $\sigma \approx 10^{-3}$ S cm^{-1}). While we have been unable to resolve the severe disorder encountered in the structure determination of [**5**][AlCl$_4$], the full characterization of related derivatives is currently underway.

Experimental Section

Starting Materials and General Procedures. Sulfur monochloride, selenium, aluminum chloride, iodobenzene, and triphenylantimony were obtained commercially (Aldrich), as was chlorine and sulfur dioxide (Matheson). Selenium tetrachloride,[20] iodobenzene dichloride,[21] and diaminobenzenedithiol dihydrochloride[22] (DADT·2HCl) were prepared according to literature procedures. Chlorobenzene (Fisher), acetonitrile

(17) (a) Kong, J.; Eriksson, L. A.; Boyd, R. J. *Chem. Phys. Lett.* **1994**, *217*, 24. (b) Martell, J. M.; Eriksson, L. A.; Goddard, J. D. *Acta Chem. Scand.* **1997**, *51*, 229.
(18) Lichtenberger, D. L.; Johnston, R. L.; Hinkelmann, K.; Suzuki, T.; Wudl, F. *J. Am. Chem. Soc.* **1990**, *112*, 3302.
(19) Bard, A. J.; Faulkner, L. R. *Electrochemical Methods*; J. Wiley and Sons: New York, 1980.
(20) Brauer, G. *Handbook of Preparative Inorganic Chemistry*; Academic Press: New York, 1963; Vol. 1, p 423.
(21) Lucas, H. J.; Kennedy, E. R. *Org. Synth. Coll. Vol. 3* **1955**, 482.
(22) Wolfe, J. F.; Loo, B. L.; Arnold, F. E. *Macromolecules* **1981**, *14*, 915.

(Fisher HPLC grade), and benzonitrile (Aldrich) were purified by distillation from P$_2$O$_5$, and thionyl chloride (Fisher) by distillation from linseed oil. All reactions were carried out under an atmosphere of nitrogen, save those involving the use of liquid sulfur dioxide (prepurified by distillation from P$_2$O$_5$), which were performed *in vacuo* using standard H-cell techniques. Fractional sublimations of **5** and **6** were performed in an ATS series 3210 three-zone tube furnace, linked to a series 1400 temperature control system. Elemental analyses were performed by MHW Laboratories, Phoenix, AZ. Infrared spectra were recorded (at 2 cm^{-1} resolution on Nujol mulls) on a Nicolet 20SX/C infrared spectrometer. Mass spectra were recorded on a Kratos MS890 mass spectrometer, using conventional direct probe EI techniques. X-band ESR spectra were recorded on a Varian E-109 spectrometer with DPPH as a field marker. UV−visible spectra were recorded on a Perkin-Elmer Lambda 6 spectrophotometer.

Preparation of 5. DADT·2HCl (0.500 g, 2.04 mmol) was heated to reflux in 10 mL of neat sulfur monochloride for 4 h. The mixture was cooled, and the black precipitate of crude [**5**][Cl] filtered off, washed with 3 × 20 mL chlorobenzene, and dried *in vacuo*. The crude [**5**][Cl] was reduced with excess triphenylantimony (0.50 g, 1.40 mmol) in refluxing acetonitrile for 30 m. A black solid was filtered off and crystallized from 150 mL of hot chlorobenzene to give purple/black microcrystals of **5** (0.30 g, 0.92 mmol, 49%). Further purification by gradient sublimation over the temperature range 150−80 °C/10^{-3} Torr afforded lustrous black needles, dec > 290 °C. IR: ν = 1495 (s), 1287 (w), 1152 (s), 959 (w) 785 (w), 777 (vs), 706 (s), 646 (m), 541 (w), 476 (w) cm^{-1}; UV/Vis (CHCl$_3$): λ_{max} (ϵ) = 522 (4 × 10^4) nm; MS (70 eV): *m/z* (%) 298 (100, [M]$^+$), 263 (9, [M − Cl]$^+$), 228 (4, [M − 2Cl]$^+$). Anal. Calcd for C$_6$Cl$_2$N$_2$S$_4$: C, 24.08; N, 9.36. Found: C, 23.99, N, 9.16.

Preparation of [5][AlCl$_4$]. Crude [**5**][Cl] (1.14 g, 3.42 mmol) and AlCl$_3$ (0.603 g, 4.45 mmol) were added to one arm of an H-cell, and 20 mL of SO$_2$(l) condensed into the flask. The dark brown mixture was stirred for 30 m and then filtered, and the black precipitate was back-washed with 3 × 5 mL SO$_2$(l). After removal of the solvent the crude product (1.16 g) was removed and extracted with SO$_2$(l) using an sealed Soxhlet extractor.[23] The solid material recovered from this extraction (0.39 g, 0.80 mmol, 23% based on crude [**5**][Cl]) showed a very clean (*vide infra*) infrared spectrum for [**5**][AlCl$_4$]. Limited quantities of crystalline black blocks suitable for analytical purposes were obtained by slow evaporation of a saturated solution in SO$_2$(l). IR (Nujol): ν = 1435 (s), 1405 (s), 1318 (w), 1299 (w), 1170 (s), 817 (s), 737 (m), 661 (m), 553 (w), 491 (br, vs) cm^{-1}. Anal. Calcd for C$_6$Cl$_6$Al$_2$N$_2$S$_4$: C, 15.40; N, 5.99. Found: C, 15.60; N, 5.78.

Preparation of [5][AlCl$_4$]$_2$. A mixture of crude [**5**][Cl] (0.334 g, 1.00 mmol), excess AlCl$_3$ (0.533 g, 4.00 mmol), and PhICl$_2$ (0.277 g, 1.00 mmol) were slurried together and heated to gentle reflux under N$_2$ in 20 mL of SOCl$_2$. After 16 h, a green precipitate of [5][AlCl$_4$]$_2$ was filtered off, washed with SOCl$_2$, and dried *in vacuo* (0.52 g, 0.82 mmol, 82% based on crude [**5**][Cl]). Crystals of [**5**][AlCl$_4$]$_2$ suitable for X-ray work were obtained by adding AlCl$_3$ to a slurry of crude [**5**][AlCl$_4$]$_2$ in SO$_2$(l) in one arm of an H-cell. The dark green solution so formed was then transferred to the other arm, which contained neat SOCl$_2$. Dark red/green plates (dec > 300 °C) grew on standing. IR (Nujol): ν =1340 (w), 1293 (s) 1194 (m), 858 (m), 842 (m), 751 (w), 669 (w), 562 (w), 521 (w), 500 (vs), 467 (s) cm^{-1}. Anal. Calcd for C$_6$Cl$_{10}$Al$_2$N$_2$S$_4$: C, 11.32, N, 4.40. Found C, 11.22, N, 3.92.

Preparation of 6. DADT·2HCl (1.00 g, 4.08 mmol) and selenium tetrachloride (2.20 g, 9.96 mmol) were heated together at reflux in 40 mL of chlorobenzene for 18 h. The mixture was then cooled and filtered, and the crude [**6**][Cl] washed with 3 × 20 mL chlorobenzene and dried *in vacuo*. This material was reduced with excess triphenyl-antimony (1.00 g, 2.80 mmol) in refluxing acetonitrile for 30 m. A black solid was filtered off and extracted with 3 × 500 mL hot benzonitrile. These extracts were combined, concentrated, and cooled to afford golden green microcrystals of **6** (0.75 g, 1.9 mmol, 49%). Further purification by gradient sublimation over the temperature range 190−100 °C/10^{-3} Torr afforded golden green blocks, mp 289 °C. IR: ν = 1486 (m), 1280 (w), 933 (w), 792 (w), 763 (m), 700 (w), 650 (w), 623 (vs), 499 (w) cm^{-1}. UV/vis (CHCl$_3$): λ_{max} (ϵ) = 536 (4 × 10^4) nm; MS (70 eV): m/z (%) 394 (100, [M]$^+$), 346 (90, [M − CCl]$^+$),

298 (26, $[M - SeN]^+$). Anal. Calcd for $C_6Cl_2N_2S_2Se_2$: C, 18.34; N, 7.13. Found: C, 18.54, N, 7.39.

Preparation of [6][AlCl$_4$]$_2$. This compound was prepared as described above for [**5**][AlCl$_4$]$_2$ (yields ca. 90% based on crude [**6**]- [Cl]). Crystals suitable for analytical and X-ray work were obtained by adding AlCl$_3$ to a slurry of crude [**6**][AlCl$_4$]$_2$ in SO$_2$(l) in one arm of an H-cell. The dark green solution so formed was then transferred to the other arm, which contained neat SOCl$_2$. Lustrous black blocks (dec > 300 °C) grew on standing. IR (Nujol): ν = 1325 (w), 1297 (s), 1187 (m), 792 (s), 667 (w), 493 (br, vs), 426 (w) cm^{-1}. Anal. Calcd for $C_6Cl_{10}Al_2N_2S_2Se_2$: C, 9.86; N, 3.83. Found: C, 9.73; N, 3.56.

Cyclic Voltammetry. Cyclic voltammetry was performed on a PAR 273A electrochemical system (EG&G Instruments) with scan rates 50– 100 mV s^{-1} on saturated solutions of **5** (0.1 M tetra-*n*-butylammonium hexafluorophosphate) in acetonitrile. Compound **6** was insufficiently soluble to allow measurements. Potentials were scanned from −2.0 to 2.5 V with respect to the quasireference electrode in a single compartment cell fitted with platinum electrodes and referenced to the ferrocenium/ferrocene couple at 0.38 V *vs* SCE.[24]

X-ray Measurements. All X-ray data were collected on an Enraf- Nonius CAD-4 diffractometer with monochromated Mo Kα radiation. Crystals were mounted on a glass fiber with silicone or embedded in epoxy. Data were collected using the θ–2θ technique. The structures were solved using direct methods and refined by full-matrix least squares analysis which minimized $\sum w(\Delta F)^2$. Crystals of **6** are twinned as a result of the β cell parameter being close to 90°. The structure was refined using the twinning feature of SHELXL-93. The crystal reported in this paper had a twin ratio of 0.70:0.30. Data sets were collected for four crystals; all were twinned with twin ratios which varied from 0.80:0.20 to 0.70:0.30. In all cases the *R*-factor before use of the twinning parameter was 20%, and after use of the twinning procedure was 8–9%. We attribute the relatively high final *R*-value to minor effects of the twinning which were not covered by this treatment.

***Ab Initio* Calculations.** All calculations were run on Silicon Graphics workstations using the B3LYP DFT method as found in the Gaussian 94 suite of programs.[25] For geometry optimizations, we used dcep-31g*, a DFT optimized core potential split valence basis set with polarization functions, as developed in our laboratories.[26] For charges, spin densities, and hyperfine coupling constants, single point B3LYP/ IGLO-III//B3LYP/dcep-31g* calculations were used. The basis set IGLO-III[27] can be described as a decontracted triple-ζ plus polarization basis, especially tailored for magnetic properties. All minima were characterized by frequency calculations. For the neutral molecule **4**, and also its radical cation [**4**]$^+$ and dication [**4**]$^{2+}$, C_{2h} symmetry was maintained. Optimization of the radical anion [**4**]$^-$ caused a major structural reorganization resulting in symmetry lowering to C_1. Spin contamination was not great, with doublets ranging from $S^2 = 0.776$ to 0.815 and triplets ranging from 2.010 to 2.014.

Supporting Information Available: Tables of crystal data, structure solution and refinement, atomic coordinates, bond lengths and angles, and anisotropic thermal parameters for **5**, [**5**][AlCl$_4$]$_2$, **6**, and [**6**][AlCl$_4$]$_2$ (14 pages). See any current masthead page for ordering and Internet access instructions.

JA972927D

(23) Small, R. W. H.; Banister, A. J.; Hauptman, Z. V. *J. Chem. Soc., Dalton Trans.* **1984**, 1377.

(24) Boeré, R. T.; Moock, K. H.; Parvez, M. Z. *Anorg. Allgem. Chem.* **1994**, *620*, 1589.

(25) Gaussian 94, Revision B.1; Frisch, M. J.; Trucks, G. W.; Schlegel, H. B.; Gill, P. M. W.; Johnson, B. G.; Robb, M. A.; Cheeseman, J. R.; Keith, T.; Petersson, G. A.; Montgomery, J. A.; Raghavachari, K.; Al-Laham, M. A.; Zakrzewski, V. G.; Ortiz, J. V.; Foresman, J. B.; Cioslowski, J.; Stefanov, B. B.; Nanayakkara, A.; Challacombe, M.; Peng, C. Y.; Ayala, P. Y.; Chen, W.; Wong, M. W.; Andres, J. L.; Replogle, E. S.; Gomperts, R.; Martin, R. L.; Fox, D. J.; Binkley, J. S.; Defrees, D. J.; Baker, J.; Stewart, J. P.; Head-Gordon, M.; Gonzalez, C.; Pople, J. A. Gaussian, Inc.: Pittsburgh, PA, 1995.

(26) Davis, W. M. Ph.D. Thesis, University of Guelph, 1996.

(27) Kutzelnigg, W.; Fleischer, U.; Schindler, M. In NMR–Basic Principles and Progress; Springer-Verlag: Heidelberg, 1990; Vol. 23, p 165–262.